

Time-asymmetric quantum-state-exchange mechanism

Ido Gilary,^{1,*} Alexei A. Mailybaev,^{2,†} and Nimrod Moiseyev^{1,3,‡}

¹*Schulich Faculty of Chemistry, Technion-Israel Institute of Technology, Haifa, 32000, Israel*

²*Instituto Nacional de Matemática Pura e Aplicada–IMPA, Estrada Dona Castorina 110, 22460-320 Rio de Janeiro, RJ, Brazil*

³*Faculty of Physics, Technion-Israel Institute of Technology, Haifa, 32000, Israel*

(Received 26 December 2012; revised manuscript received 10 April 2013; published 25 July 2013)

We show here that due to nonadiabatic couplings in decaying systems, applying the same time-dependent protocol in the forward and reverse direction to the same mixed initial state leads to different final pure states. In particular, in laser-driven molecular systems, applying a specifically chosen positively chirped laser pulse or an equivalent negatively chirped laser pulse yields entirely different final vibrational states. This phenomenon occurs when the laser frequency and intensity are slowly varied around an exceptional point (EP) in the laser intensity and frequency parameter space where the non-Hermitian spectrum of the problem is degenerate. The protocol implies that a positively chirped laser pulse traces a loop in time in the laser parameters' space whereas a negatively chirped pulse follows the same loop in the opposite direction. According to this protocol one can choose the final pure state from any initial state. The obtained results imply the intrinsic nonadiabaticity of quantum transport around an EP, and offer a way to observe the EP experimentally in time-dependent quantum systems.

DOI: [10.1103/PhysRevA.88.010102](https://doi.org/10.1103/PhysRevA.88.010102)

PACS number(s): 03.65.Vf, 37.90.+j

One of the basic properties of quantum mechanics is that the Hamiltonian of a given system is Hermitian and its energies are real. This is important in the context of describing bound states, but in open quantum systems where particles can decay, metastable states can form. Non-Hermitian (NH) quantum mechanics (NHQM) has been an efficient tool to describe such systems ever since the pioneering work of Gamow [1] and Siegert [2] in tackling the problem of nuclear decay. NH Hamiltonians come about in a variety of ways which are often due to the reduction of the physical problem to an effective Hamiltonian describing a restricted part of the system. For a detailed account of how NH Hamiltonians are obtained and the physical meaning of the complex energies, see Ref. [3].

For open quantum systems where the effective Hamiltonian is NH, the noncrossing rule [4] is replaced by an intersection of two complex energy levels associated with two eigenfunctions of the NH Hamiltonian that have the same symmetry. Let us consider the 2×2 Hamiltonian matrix H which depends on potential parameters q_1 and q_2 . These can be, for instance, the laser frequency and intensity when light interacts with two normal modes of a molecule.

In an open quantum system, where the effective Hamiltonian is NH, all matrix elements can attain complex values. The complex diagonal matrix elements are associated with metastable (resonance) states, such that $-2\text{Im}[H_{11}]$ and $-2\text{Im}[H_{22}]$ are the decay rates of the metastable states. The eigenvalues of this NH Hamiltonian are degenerate when $\Delta = (H_{11} - H_{22})^2 + 4H_{12}H_{21} = 0$ even though all matrix elements are different from zero. This situation is very different from the Hermitian (standard) case where crossing requires $H_{12} = H_{21} = 0$ and $H_{11} = H_{22}$. At the crossing point a non-Hermitian degeneracy (NHD) is obtained when the following

two equations are satisfied:

$$\text{Re}[H_{11} - H_{22}] = \mp 2 \text{Im}[H_{12}H_{21}]^{1/2}, \quad (1)$$

$$\text{Im}[H_{11} - H_{22}] = \pm 2 \text{Re}[H_{12}H_{21}]^{1/2}. \quad (2)$$

NHD is very different in its nature from Hermitian degeneracy. NHD is obtained at the crossing point denoted by $(q_1^{\text{EP}}, q_2^{\text{EP}})$, where the two eigenvalues coalesce and form a branch point also known as an exceptional point (EP) in the complex energy spectrum [5,6]. At the EP the first-order derivatives of the eigenvalues with respect to q_1 or q_2 acquire infinitely large values (see, for example, Chap. 9 in Ref. [3]). Moreover, at the EP, not only do the eigenvalues coalesce but also the corresponding eigenvectors. Such a phenomenon can never occur in standard QM. In NHQM, as $q_1 \rightarrow q_1^{\text{EP}}$ and $q_2 \rightarrow q_2^{\text{EP}}$, the two biorthogonal eigenvectors of the complex non-Hermitian Hamiltonian matrix coalesce. Rather than two different biorthogonal eigenvectors, we get only one eigenvector which is self-orthogonal (with respect to the c product) [7,8]. As proved in Refs. [9,10], EPs are a common feature phenomenon in NHQM.

In the past decade it became clear that EPs are not only mathematical objects but they play a major role also in actual measurable phenomena. Different manifestations of EPs have been described in a variety of fields [11–16]. So far experimental results regarding EPs in atomic, molecular, or biophysical systems are lacking.

Before proceeding we should mention the most striking phenomenon induced by EPs which has no equivalent in Hermitian QM: the state-exchange phenomenon. The state-exchange phenomenon can be illustrated as follows: Consider an arbitrary variation of the two parameters (q_1, q_2) which depend on angle variable φ in a closed loop around an EP $(q_1^{\text{EP}}, q_2^{\text{EP}})$. The two instantaneous eigenvalues are given by

$$E_{\pm}(\varphi) = \frac{H_{11} + H_{22} \pm \sqrt{\Delta(\varphi)}}{2}, \quad (3)$$

*chgilary@tx.technion.ac.il

†alexei@impa.br

‡nimrod@tx.technion.ac.il

where the quantity $\Delta(\varphi)$ makes a circle around the origin in the complex plane with a change of φ . Thus, it is easy to see that $E_{\pm}(0) = E_{\mp}(2\pi)$. Instead of the Berry phase, which is obtained when cycling around a conical intersection, when cycling around an EP one state flips into the other (see Chap. 9 in Ref. [3]). To the best of our knowledge the only measurement of this phenomenon was carried out by Richter and co-workers in microwave experiments [14]. The association of the state-exchange phenomenon with a molecular system was made by Lefebvre and co-workers [17].

The model 2×2 Hamiltonian matrix which was discussed above can describe, in the NH case, two coupled resonance states, where H_{11} is the complex energy of the atomic, molecular, or mesoscopic resonance state that absorbed one photon, $H_{11} = E_1 - i\Gamma_1 + \hbar\omega$, while $H_{22} = E_2 - i\Gamma_2$ is the complex energy of the excited resonance state. $\Gamma_1 > 0$ and $\Gamma_2 > 0$ are the decay rates of the two resonance states. The coupling term as usual is given by $H_{12} = H_{21} = \epsilon_0 d_{12}/2$, where ϵ_0 is the maximum laser field amplitude and d_{12} is the complex dipole transition-matrix element. The NH Hamiltonian matrix can be now rewritten such that

$$H = \begin{pmatrix} E_1 + \hbar\omega + \frac{i\Delta\Gamma}{2} & \frac{\epsilon_0 d_{12}}{2} \\ \frac{\epsilon_0 d_{12}}{2} & E_2 - \frac{i\Delta\Gamma}{2} \end{pmatrix} - i \frac{\Gamma_1 + \Gamma_2}{2} \begin{pmatrix} 1 & 0 \\ 0 & 1 \end{pmatrix}, \quad (4)$$

where $\Delta\Gamma = \Gamma_2 - \Gamma_1$. As one can see from Eq. (4), relative gain and loss states are obtained (e.g., when $\Delta\Gamma > 0$, then one state has a relative gain while the other resonance state has a relative loss). EP is obtained when Eqs. (1) and (2) are satisfied. Consequently, an EP in the spectrum is obtained when the maximum field amplitude is $\epsilon_0^{\text{EP}} = \Delta\Gamma/\text{Re}[d_{12}]$ and the laser frequency is equal to $\omega^{\text{EP}} = (E_2 - E_1 - \text{Im}[d_{12}]\epsilon_0^{\text{EP}})/\hbar$. When the laser field is strong enough to allow a multiphoton absorption, the calculations of the conditions for EP are slightly more complicated but achievable.

In closed systems adiabatic solutions converge to the exact solutions of the time-dependent Schrödinger equation (TDSE) in the limit of infinitely slow variation of the potential parameters. In contrast, in open systems for almost any path in parameter space, the nonadiabatic couplings become more significant as the potential parameters are varied slower. As a result, the adiabatic theorem often breaks down in open quantum systems. Let us explain this for our 2×2 model Hamiltonian when the two potential parameters q_1 and q_2 are time-dependent parameters. These can be external field parameters such as laser frequency and intensity. The conventional adiabatic approximation is associated with the eigenvalues $E_{\pm}^{\text{ad}}(q_1, q_2)$ and eigenfunctions $\phi_{\pm}^{\text{ad}}(q_1, q_2)$ of the Hamiltonian matrix in Eq. (4). The dynamical nonadiabatic corrections to the solutions of the TDSE result from the dependence of the potential parameters q_1 and q_2 on time. These couple different adiabatic states and are given by the following matrix elements,

$$\begin{aligned} V_{+/-}^{\text{NA}} &= \mathcal{V}_{+/-} e^{+i \int_0^T \Delta E^{\text{ad}}[q_1(t), q_2(t)] dt}, \\ V_{-/+}^{\text{NA}} &= \mathcal{V}_{-/+} e^{-i \int_0^T \Delta E^{\text{ad}}[q_1(t), q_2(t)] dt}, \end{aligned} \quad (5)$$

where

$$\begin{aligned} \mathcal{V}_{+/-} &= \langle \phi_+^{\text{ad}}(q_1, q_2) | \dot{q}_1 \frac{\partial}{\partial q_1} + \dot{q}_2 \frac{\partial}{\partial q_2} | \phi_-^{\text{ad}}(q_1, q_2) \rangle, \\ \mathcal{V}_{-/+} &= \langle \phi_-^{\text{ad}}(q_1, q_2) | \dot{q}_1 \frac{\partial}{\partial q_1} + \dot{q}_2 \frac{\partial}{\partial q_2} | \phi_+^{\text{ad}}(q_1, q_2) \rangle, \end{aligned} \quad (6)$$

and

$$\begin{aligned} \Delta E^{\text{ad}}(q_1, q_2) &= E_+^{\text{ad}}(q_1, q_2) - E_-^{\text{ad}}(q_1, q_2) \\ &\equiv \Delta \mathcal{E}^{\text{ad}}(q_1, q_2) - i \Delta \Gamma^{\text{ad}}(q_1, q_2). \end{aligned} \quad (7)$$

Here T is the duration of the loop in the parameter space. For closed systems where the Hamiltonian is Hermitian, $\Delta E^{\text{ad}}(q_1, q_2)$ has real values only. Therefore the exponents in Eq. (5) are just a phase factor, and the nonadiabatic corrections vanish as $T \rightarrow \infty$ (i.e., the variation of the potential parameters is arbitrarily slow).

In an open system where we are dealing with resonances, the energy difference might be complex. The imaginary part of the energy difference, $\Delta \Gamma^{\text{ad}} > 0$, for instance, leads to $V_{+/-}^{\text{NA}} \rightarrow \infty$ while $V_{-/+}^{\text{NA}} \rightarrow 0$ as $T \rightarrow \infty$. The exponential divergence in T of the exponent in $V_{+/-}^{\text{NA}}$ easily overcomes the $1/T$ suppression (responsible for the Hermitian adiabatic theorem) that is associated with the preexponential terms in Eq. (5) that contain the time derivatives of the potential parameters $\dot{q}_{1,2}$. This implies that in the limit of slow evolution only one state evolves adiabatically while the other state behaves nonadiabatically. The adiabatic state is the one which decays slower. For other states the adiabatic solution is not valid even approximately, making the adiabatic flip often discussed in the literature [17, 18] impossible.

Let us assume that our protocol implies that the external potential parameters (q_1, q_2) are varied in time in a closed loop which encircles the EP (see, for example, Fig. 1). This EP is obtained at the values $(q_1^{\text{EP}}, q_2^{\text{EP}})$ of the external parameters. Note that this dynamical protocol requires to solve the

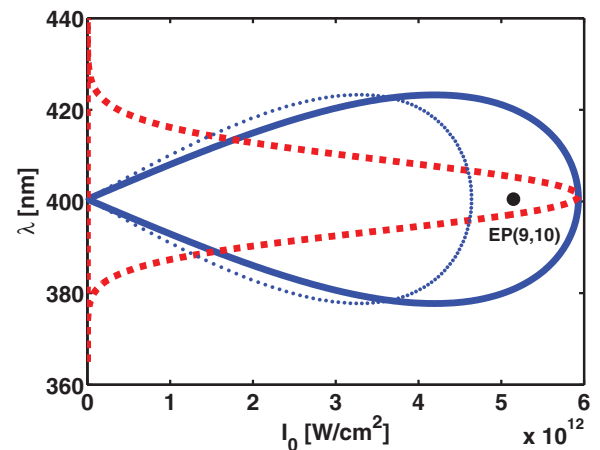


FIG. 1. (Color online) Loops in the parameter space of the laser intensity and wavelength. When the laser intensity is turned on, the ninth and the tenth vibrational states of the molecular ion become resonances. The EP is obtained when the two resonances become degenerate non-Hermitian eigenstates. Note that the red dashed line representing a chirped Gaussian laser pulse closes a loop on the zero intensity axis.

time-dependent Schrödinger equation. The only adiabatic solution which describes correctly the dynamics is the longest-lived resonance state. The lifetimes of the adiabatic resonance states are obtained by averaging the decay rates over the entire closed loop in the potential parameter space. That is, the inverse lifetime of the adiabatic states denoted by \pm are given by $T^{-1} \int_0^T \Gamma_{\pm}^{\text{ad}} dt$, where Γ_{\pm}^{ad} is the decay rate at any given point on the closed loop.

A key point in understanding the difference between the dynamics for bound and decaying systems is to realize how the nonadiabatic dynamical correction terms couple different adiabatic solutions. There is an asymmetric phenomenon in the strength of the dynamical nonadiabatic coupling between two adiabatic resonance solutions which does not exist between two bound adiabatic solutions. The strength of the nonadiabatic coupling term that induces a transition from the $|\phi_{+}^{\text{ad}}\rangle$ state to the $|\phi_{-}^{\text{ad}}\rangle$ state is proportional to $e^{-\int_0^T \Delta\Gamma^{\text{ad}} dt}$ while the strength of the coupling that induces the transition from the $|\phi_{-}^{\text{ad}}\rangle$ to the $|\phi_{+}^{\text{ad}}\rangle$ adiabatic resonance solution is the inverse of this expression, i.e., $e^{+\int_0^T \Delta\Gamma^{\text{ad}} dt}$ [see Eqs. (5)–(7)]. This asymmetric dynamical nonadiabatic effect stands behind our discovery that at the end of the propagation the system is found in the longest-lived pure state, irrespective of the initial condition. This effect is not due to the “evaporation” of the shorter-lived adiabatic states. It happens because the short-lived adiabatic states are transformed into the long-lived adiabatic states during propagation. This phenomenon was first described in Ref. [19]. In Ref. [20] this state-exchange phenomenon was illustrated for a real physical system of H_2^+ interacting with chirped laser pulses.

We are now at the core of the universal asymmetric state-exchange phenomenon which is the focus of this study. It is based on the observation that the integral $\int_0^T \Delta\Gamma^{\text{ad}} dt$ changes sign when the loop in parameter space changes from the clockwise direction to the counterclockwise direction if the closed loop encircles an EP (this is due to the exchange of the instantaneous states which is the property of the EP described above). This means that the dynamical protocol described above imposes specific asymmetry for our time-dependent Hamiltonian. The consequences are dramatic. By applying the dynamical protocol in the clockwise direction, the $|\phi_{+}^{\text{ad}}\rangle$ state is obtained, as the external parameters return to their initial values (independently of the initial state). The $|\phi_{-}^{\text{ad}}\rangle$ state will be obtained when the same protocol is applied in the counterclockwise direction. This way we can control the dynamics and produce a quantum diodelike device for atomic, molecular, or optical systems, such that the output depends on the direction in which one enters the device.

To illustrate and confirm the possibility of a diodelike quantum gate by applying the nonadiabatic time-asymmetric (NA-TAS) mechanism, we apply the above protocol to H_2^+ in a laser field characterized by its wavelength λ and intensity I_0 or, alternatively, by its frequency ω and amplitude ϵ_0 . We chose this system since it was a subject of experimental studies for many years (see, for example, Ref. [21]) and since our theoretical predictions can be experimentally confirmed.

In the spirit of Eq. (4), we use the formalism described in Ref. [20] where the radiation introduces a time-dependent

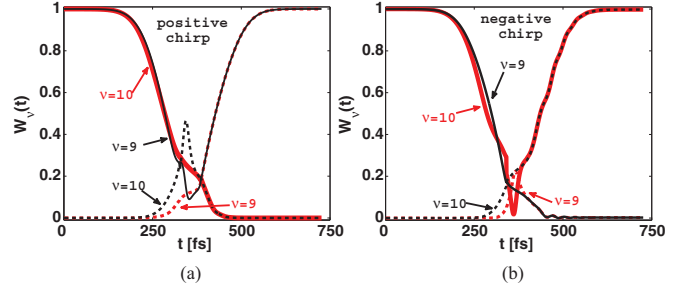


FIG. 2. (Color online) The asymmetric state-exchange mechanism in H_2^+ . $W_v(t)$ is the projection of the propagated H_2^+ wave packet (WP) during a chirped Gaussian laser pulse on the field-free vibrational states of the molecular ions, $\nu = 9$ and $\nu = 10$. The thin black lines describe the solution which starts at the $\nu = 9$ vibrational state whereas the thick red lines describe the solution which starts at the $\nu = 10$ vibrational state. The chirp changes the laser wavelength and intensity in time according to the dashed red loop encircling the EP shown in Fig. 1. (a) A positive chirp corresponds to a clockwise trajectory on the loop. (b) A negative chirp corresponds to a counterclockwise trajectory on the loop. Similar results are obtained when we follow a trajectory along the blue solid line in Fig. 1.

coupling between the ground and excited electronic states of the molecular ion system. We assume that the whole effect of the laser field is to bring the bound vibrational states of the ground electronic state $[E_g(R)]$ up by one photon energy and couple it with the continuum of the excited electronic state $[E_e(R)]$ through the dipole $d(R)$. This leads to following effective Hamiltonian:

$$\hat{H}(R; t) = \begin{pmatrix} \hat{T}(R) + E_g(R) + \hbar\omega(t) & \frac{\epsilon_0(t)d(R)}{2} \\ \frac{\epsilon_0(t)d(R)}{2} & \hat{T}(R) + E_e(R) \end{pmatrix}. \quad (8)$$

Here R is the internuclear distance, $\hat{T}(R)$ is the nuclear kinetic energy operator, and the functional dependence of $E_{g,e}(R)$ and $d(R)$ is given in Ref. [22]. Since the bound vibrational states of the ground electronic potential interact with the scattering states of the excited electronic potential in which they are embedded, they become metastable. The resonance energies are obtained by the complex scaling method [7]. The numerical results were obtained by propagating the system from $t = 0$ by using the Runge-Kutta method where in each time step the wave function is expanded in the basis of the instantaneous solutions of Eq. (8).

Figure 2 demonstrates the interaction of H_2^+ with a chirped Gaussian envelope laser pulse according to two different protocols shown in Fig. 1 by the red dashed line. Figure 2(a) displays the results of a positive chirp which follows the dashed line in Fig. 1 in the clockwise direction while Fig. 2(b) shows the results of a negative chirp which traverses the same loop but in the counterclockwise direction. In both cases the pulse is centered around 401 nm, the pulse duration is 164.5 fs, the chirp rate is $1.3 \times 10^{-3} \text{ fs}^{-2}$, and the peak intensity is $5.9 \times 10^{12} \text{ W/cm}^2$. Note that in these calculations we normalized the propagated wave packet (WP) to unity at any given time in order to compensate for the decay.

TABLE I. The driven asymmetric effect on the state-to-state vibrational transitions of H_2^+ when either positive or negative chirp laser pulses are used. In a separate column we show that the adiabatic approximation yields an incorrect prediction for the final state. In both cases the laser parameters are varied in a closed loop which encircles the EP shown in Fig. 1.

	Initial	Final (adiabatic)	Final (exact)
↻	$ 9\rangle$	$ 10\rangle$	$ 9\rangle$
	$ 10\rangle$	$ 9\rangle$	$ 9\rangle$
↺	$ 9\rangle$	$ 10\rangle$	$ 10\rangle$
	$ 10\rangle$	$ 9\rangle$	$ 10\rangle$

The results of Fig. 2 can be summarized in Table I to illustrate how by going along a loop in one direction we always obtain one of the coalescing states, whereas by going in the other direction we will always wind up in the other state. This result is independent of the initial superposition of the two field-free states. These results clearly demonstrate the power of the mechanism proposed in this research, with the purpose to induce asymmetric transition which is caused by a nonadiabatic interaction between metastable states.

What is missing in this representation is the fact that the NA-TAS mechanism is not only very efficient in producing asymmetric molecular diodelike device but can also be achieved at smaller pulse times, which can reduce the number of molecules that dissociate during the interaction with the laser and thus increase the population which survives in the desired state by the end of the pulse.

In order to illustrate this important property of the NA-TAS mechanism, we present below the dependence of the surviving population in each of the field-free states on the duration of the laser pulse. The path we trace in the laser parameters space follows the solid and dotted loops in Fig. 1. These loops are of the form $I(\tau) = I_0 \sin(\tau/2)$, $\lambda = \lambda_0 + \delta \sin \tau$, where $\tau = 2\pi t/T_{\text{loop}}$. The angular dependence of the wavelength λ and laser intensity insures that these loops trace the same path in parameter space when we change the duration of the pulse T_{loop} . The solid-line loop encircles the EP marked by the circle on Fig. 1 whereas the dotted-line loop does not.

In Fig. 3 we show the population in the ninth and tenth vibrational states of H_2^+ at the end of the laser pulse as a function of the pulse duration T_{loop} . The initial state in all cases is an equal weight superposition of the two states. Figure 3(a) shows the results for a clockwise path along the loops while Fig. 3(b) gives the results of a counterclockwise path along the loops.

It is evident from the results of Fig. 3 that, by encircling an EP, a better separation between the final populations of the two states occurs. This separation is also obtained at a much shorter pulse duration, thus enabling to achieve a desired state with a significant number of undissociated molecules remaining.

Figure 3 demonstrates that due to the nonadiabatic couplings of Eq. (5), whenever we wait long enough, a separation between the surviving population of the two states will occur.

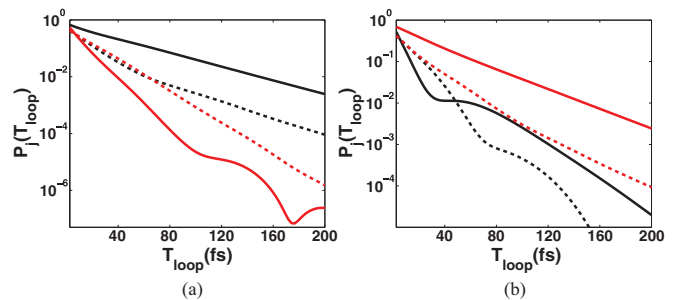


FIG. 3. (Color online) The population P_j of the ninth (black) and tenth (red) vibrational states of H_2^+ at the end of the laser pulse on a logarithmic scale as a function of the pulse duration T_{loop} . The solid lines correspond to the solid-line loop in Fig. 1, which encircles the EP, while the dashed lines correspond to the dotted-line loop in Fig. 1, which excludes the EP. The initial state for all calculations is an equal weight superposition of the two states. (a) displays the results of the clockwise path on the loops while (b) portrays the results of the counterclockwise path on the loops.

This is obviously due to the difference in the decay rates of the instantaneous solutions. In general, the state which survives and the duration of the pulse required to reach separation strongly depend on the loop parameters. However, by encircling an EP we have a means to ensure that we achieve clear separation and to choose the desired resulting state by the NA-TAS mechanism. In order for the instantaneous solutions to exchange, when we encircle the EP adiabatically, one solution must have a decay rate larger than that at the EP while the decay rate of the other solution must be smaller. This makes the NA-TAS protocol around the EP presented here very effective and controlled. It is also robust since it will be applicable in any physical system where an EP occurs (i.e., any system open to decay).

Here we showed that there are observable physical phenomena which are hard to predict by Hermitian quantum mechanics but can be readily explained and predicted by using the theoretical tools developed within the framework of non-Hermitian quantum mechanics. Moreover, the time-asymmetric state-exchange mechanism, which is based on our ability to locate non-Hermitian degeneracies, enables one to control the dynamics by external parameters of the fields with which the system under study interacts. This may open a door to different types of technologies, to other types of photo-switches, diodelike atomic, molecular, and optical devices. For instance, the propagation of leaky modes in waveguides is often described by a non-Hermitian operator. The relevant control parameter in this case is the index of refraction of the materials comprising the waveguide. Applying the scheme we presented here to such a system may allow the fabrication of a device which yields an output signal based on the direction one enters the device, regardless of the input signal.

ISF (Grant No. 298/11) and CNPq (Grant No. 305519/2012-3) are acknowledged for their support. A.M. is grateful for the hospitality and support during his stay in Technion.

- [1] G. A. Gamow, *Z. Phys.* **51**, 204 (1928).
- [2] A. J. F. Siegert, *Phys. Rev.* **56**, 750 (1939).
- [3] N. Moiseyev, *Non-Hermitian Quantum Mechanics* (Cambridge University Press, Cambridge, UK, 2011).
- [4] J. von Neumann and E. P. Wigner, *Phys. Z.* **30**, 467 (1929).
- [5] T. Kato, *Perturbation Theory of Linear Operators* (Springer, Berlin, 1966).
- [6] W. D. Heiss and H. L. Harney, *Eur. Phys. J. D* **17**, 149 (2001).
- [7] N. Moiseyev, *Phys. Rep.* **302**, 211 (1998).
- [8] N. Moiseyev, P. R. Certain, and F. Weinhold, *Mol. Phys.* **36**, 1613 (1978).
- [9] V. I. Arnold, *Geometrical Methods in the Theory of Ordinary Differential Equations* (Springer, New York, 1983).
- [10] N. Moiseyev and S. Friedland, *Phys. Rev. A* **22**, 618 (1980).
- [11] M. V. Berry, *Czech. J. Phys.* **54**, 1039 (2004).
- [12] J. Rubinstein, P. Sternberg, and Q. Ma, *Phys. Rev. Lett.* **99**, 167003 (2007).
- [13] P. Cejnar, S. Heinze, and M. Macek, *Phys. Rev. Lett.* **99**, 100601 (2007).
- [14] C. Dembowski, H.-D. Graf, H. L. Harney, A. Heine, W. D. Heiss, H. Rehfeld, and A. Richter, *Phys. Rev. Lett.* **86**, 787 (2001).
- [15] S. Klaiman, U. Günther, and N. Moiseyev, *Phys. Rev. Lett.* **101**, 080402 (2008).
- [16] M. Liertzer, Li Ge, A. Cerjan, A. D. Stone, H. E. Türeci, and S. Rotter, *Phys. Rev. Lett.* **108**, 173901 (2012).
- [17] R. Lefebvre, O. Atabek, M. Šindelka, and N. Moiseyev, *Phys. Rev. Lett.* **103**, 123003 (2009).
- [18] A. A. Mailybaev, O. N. Kirillov, and A. P. Seyranian, *Phys. Rev. A* **72**, 014104 (2005).
- [19] R. Uzdin, A. Mailybaev, and N. Moiseyev, *J. Phys. A* **44**, 435302 (2011).
- [20] I. Gilary and N. Moiseyev, *J. Phys. B* **45**, 051002 (2012).
- [21] U. Lev, V. Prabhudesai, A. Natan, B. Bruner, A. Diner, O. Heber, D. Strasser, D. Schwalm, I. Ben-Itzhak, J. J. Hua, B. D. Esry, Y. Silberberg, and D. Zajfman, *J. Phys.: Conf. Ser.* **194**, 032060 (2009).
- [22] F. V. Bunkin and I. I. Tugov, *Phys. Rev. A* **8**, 601 (1973).